

## Supplementary Materials for

# **Pb<sup>II</sup>-Catalyzed Transformation of Aromatic Nitriles to Heptanitrogen Anion via Sodium Azide: A Combined Experimental and Theoretical Study**

**Rong-Yi Huang,<sup>\*,a</sup> Chao Zhang,<sup>a</sup> Da Yan,<sup>a</sup> Zhi Xiong,<sup>a</sup> Heng Xu,<sup>\*,a</sup> and Xiao-Ming Ren<sup>\*,b</sup>**

*<sup>a</sup> Anhui Key Laboratory of Functional Coordination Compounds and School of Chemistry and Chemical Engineering, Anqing Normal University, Anqing 246011, P. R. China*

*<sup>b</sup> State Key Laboratory of Materials-Oriented Chemical Engineering and College of Chemistry & Molecular Engineering, Nanjing Tech University, Nanjing, 210009, P. R. China*

# Supporting Information Contents

## 1. Thermal decomposition behaviors of **MOF-N<sub>7</sub>** and **Pb-FBA**

**Table S1:** Selected bond lengths (Å) and angles (°) for **MOF-N<sub>7</sub>**.

**Table S2:** Selected bond lengths (Å) and angles (°) for **α-Pb(N<sub>3</sub>)<sub>2</sub>**.

**Table S3:** Selected bond lengths (Å) and angles (°) for **Pb-FBA**.

**Table S4:** The calculated interaction energies corrected with BSSE and ZPE,  $\Delta E_{\text{int}}$  for the associations **Pb⋯N<sub>3</sub>** and **Pb⋯4-FBN** (kcal·mol<sup>-1</sup>).

**Table S5:** Topological parameters at bond critical points of the Pb-N and N-N bonds in **MOF-N<sub>7</sub>'**.

**Fig. S1.** The calculated structures for the **Pb⋯N<sub>3</sub>** and **Pb⋯4-FBN** associations.

**Fig. S2.** The structures of the representative fragments **N<sub>7</sub><sup>3-</sup>-C<sub>2h</sub>**, **N<sub>7</sub><sup>3-</sup>-C<sub>2v</sub>**, and **MOF-N<sub>7</sub>'**.

**Fig. S3.** The XPRD patterns obtained for **MOF-N<sub>7</sub>**.

**Fig. S4.** (a) The coordination environment of the Pb<sup>2+</sup> ions in **MOF-N<sub>7</sub>** with the ellipsoids drawn at the 30% probability level. Distorted water molecules and all hydrogen atoms were omitted for clarity. (b) The 1D chain constructed via the C<sub>2</sub>O<sub>4</sub><sup>2-</sup> anions and [Pb<sub>6</sub>O<sub>2</sub>]<sup>8+</sup> cationic clusters along the *a*-axis. (c) The 1D chain constructed via the CHDA<sup>2-</sup> anions and Pb<sup>2+</sup> ions along the *a*-axis. (d) The 2D metal-organic layer parallel to the *ab* plane in **MOF-N<sub>7</sub>**. (e) The 3D open framework constructed from the 2D layers and N<sub>7</sub> anionic pillars of **MOF-N<sub>7</sub>**.

**Fig. S5.** The FT-IR spectrum obtained of **MOF-N<sub>7</sub>**.

**Fig. S6.** The coordination environment of the Pb<sup>2+</sup> ions in **α-Pb(N<sub>3</sub>)<sub>2</sub>** with the ellipsoids drawn at the 30% probability level.

**Fig. S7.** The coordination environment of the Pb<sup>2+</sup> ion in **Pb-FBA** with the ellipsoids drawn at the 30% probability level. Distorted water molecules and all hydrogen atoms were omitted for clarity.

**Fig. S8.** The ELF- $\pi$  isosurfaces (value = 0.70) of **N<sub>7</sub><sup>3-</sup>-C<sub>2v</sub>** (top) and the **N<sub>7</sub><sup>3-</sup>** polynitrogen fragment in **MOF-N<sub>7</sub>'** (bottom).

**Fig. S9.** The TGA plot obtained for **Pb-FBA** at a heating rate of  $10^{\circ}\text{C}\cdot\text{min}^{-1}$  under a flow of  $\text{N}_2$ .

### 1. Thermal decomposition behaviour of **MOF-N<sub>7</sub>** and **Pb-FBA**

To test the robustness of **MOF-N<sub>7</sub>** and **Pb-FBA**, thermogravimetric analyses (TGA) were obtained via heating the crystalline samples in the temperature range of 20 to 800 °C under a N<sub>2</sub> atmosphere (Figures 7 and S9). For **MOF-N<sub>7</sub>**, the TGA results show that the **MOF-N<sub>7</sub>** framework was stable up to approximately 369 °C and then started to abruptly decompose. The first mass loss of the four guest water molecules and one hydronium ion per formula unit occurred in range of 20 to 369 °C with a 3.5% mass loss (calc. 3.4%). The second major mass loss of the four CHDA<sup>2-</sup> ligands, one ox<sup>2-</sup> ligand and two O<sup>2-</sup> anions, occurred in range of 369 to 430 °C with a 31.5% mass loss (calc. 30.1%). The third minor weight loss of the N<sub>7</sub><sup>3-</sup> polynitrogen occurred with a 3.8% mass loss (calc. 3.7%). The percentage remaining was 61.0%, meaning that the final product was metallic lead (calc. 62.6%). In addition, the DSC curve presents three endothermic peaks at 381, 406 and 419 °C in range of 369 to 430 °C, which can be assigned to the removal of the four CHDA<sup>2-</sup> ligands, one ox<sup>2-</sup> ligand and two O<sup>2-</sup> anions, respectively. Interestingly, a larger exothermic peak was observed at 607 °C in range of 430 to 800 °C, accompanied an exothermic enthalpy change of 8.61 kJ/g, which was due to the decomposition of the N<sub>7</sub><sup>3-</sup> polynitrogen. **Pb-FBA** lost two guest water molecules from 20 to 400 °C, accompanied by a mass loss of 4.4% (calc.4.8%). After 400 °C, **Pb-FBA** started to abruptly decompose, which corresponds to the decomposition of **FBA<sup>-</sup>** and O<sup>2-</sup> anions. Up until 800 °C, **Pb-FBA** did not decompose completely.

**Table S1:**Selected bond lengths (Å) and angles (°) for **MOF-N<sub>7</sub>**.

Pb(1)–O(1)	2.314(7)	Pb(1)–O(2)	2.592(10)
Pb(1)–O(1)#1	2.314(7)	Pb(1)–O(2)#2	2.592(10)
Pb(1)–O(4)	3.029(12)	Pb(1)–N(1)	2.600(2)
Pb(1)–O(4)#2	3.029(12)	Pb(2)–O(3)	2.642(12)
Pb(2)–O(5)#3	2.562(12)	Pb(2)–O(6)#3	2.934(12)
Pb(2)–O(3)#4	2.642(12)	Pb(2)–O(6)#5	2.588(12)
Pb(2)–O(5)#6	2.562(12)	Pb(2)–O(6)#6	2.934(12)
Pb(2)–O(6)#7	2.588(12)	Pb(3)–O(1)	2.278(7)
Pb(3)–O(2)	2.731(11)	Pb(3)–O(3)	2.638(12)
Pb(3)–O(4)#4	2.438(11)	Pb(3)–N(1)#4	2.910(8)
Pb(3)–O(5)#6	2.829(12)	Pb(3)–O(3)#4	2.913(11)
N(1)–N(2)	1.198(31)	N(3)–N(4)	1.191(30)
N(2)–N(3)	1.261(39)		
N(1)–N(2)–N(3)	165.2(3)	N(3)–N(4)–N(3)#8	180.0(2)
N(2)–N(3)–N(4)	165.9(3)		
O(1)–Pb(1)–O(2)	76.8(3)	O(1)–Pb(1)–O(4)	66.8(3)
O(1)–Pb(1)–O(1)#1	75.1(3)	O(1)–Pb(1)–O(2)#2	114.4(3)
O(2)–Pb(1)–O(4)	75.9(3)	O(2)–Pb(1)–N(1)	146.7(3)
O(2)–Pb(1)–O(2)#2	63.5(4)	O(2)–Pb(1)–O(4)#2	136.8(3)
O(4)–Pb(1)–O(1)#1	137.0(3)	O(4)–Pb(1)–O(2)#2	136.8(3)
N(1)–Pb(1)–O(1)#1	75.5(4)	N(1)–Pb(1)–O(2)#2	146.7(3)
O(1)#1–Pb(1)–O(2)#2	76.8(3)	O(1)#1–Pb(1)–O(4)#2	66.8(3)
O(3)–Pb(2)–O(5)#3	68.7(4)	O(3)–Pb(2)–O(6)#3	112.8(4)
O(3)–Pb(2)–O(6)#6	90.0(3)	O(3)–Pb(2)–O(3)#4	66.3(4)
O(3)–Pb(2)–O(6)#7	91.2(4)	O(5)#3–Pb(2)–O(6)#3	44.2(4)
O(5)#3–Pb(2)–O(6)#6	152.9(4)	O(5)#3–Pb(2)–O(3)#4	74.9(4)
O(5)#3–Pb(2)–O(6)#7	95.2(4)	O(6)#3–Pb(2)–O(5)#6	152.9(4)
O(6)#3–Pb(2)–O(3)#4	90.0(3)	O(6)#3–Pb(2)–O(6)#5	67.6(4)
O(5)#6–Pb(2)–O(6)#6	44.2(4)	O(5)#6–Pb(2)–O(3)#4	68.7(4)
O(5)#6–Pb(2)–O(6)#7	109.2(4)	O(6)#6–Pb(2)–O(3)#4	112.8(4)
O(6)#6–Pb(2)–O(6)#7	67.6(4)	O(3)#4–Pb(2)–O(6)#5	91.2(4)

O(6)#5–Pb(2)–O(6)#7	111.4(4)	O(1)–Pb(3)–O(2)	74.6(2)
O(1)–Pb(3)–O(5)#6	133.4(3)	O(1)–Pb(3)–O(3)#4	73.4(3)
O(1)–Pb(3)–N(1)#4	70.0(5)	O(2)–Pb(3)–O(3)#4	134.2(3)
O(2)–Pb(3)–O(5)#6	130.8(3)	O(3)–Pb(3)–O(4)#4	110.2(4)
O(2)–Pb(3)–N(1)#4	75.2(5)	O(5)#6–Pb(3)–O(3)#4	61.5(3)
O(3)–Pb(3)–O(3)#4	62.5(3)	O(5)#3–Pb(2)–O(6)#5	109.2(4)
O(5)#6–Pb(3)–N(1)#4	144.6(5)	O(6)#3–Pb(2)–O(6)#6	153.2(3)
O(3)#4–Pb(3)–N(1)#4	121.6(5)	O(6)#3–Pb(2)–O(6)#7	96.9(4)
O(1)–Pb(1)–N(1)	75.5(4)	O(5)#6–Pb(2)–O(6)#5	95.2(4)
O(1)–Pb(1)–O(4)#2	137.0(3)	O(6)#6–Pb(2)–O(6)#5	96.9(4)
O(2)–Pb(1)–O(1)#1	114.4(3)	O(3)#4–Pb(2)–O(6)#7	157.4(4)
O(4)–Pb(1)–N(1)	76.4(3)	O(1)–Pb(3)–O(3)	79.2(3)
O(4)–Pb(1)–O(4)#2	135.1(3)	O(1)–Pb(3)–O(4)#4	78.9(3)
N(1)–Pb(1)–O(4)#2	76.4(3)	O(2)–Pb(3)–O(3)	80.0(3)
O(2)#2–Pb(1)–O(4)#2	75.9(3)	O(2)–Pb(3)–O(4)#4	149.2(4)
O(3)–Pb(2)–O(5)#6	74.9(4)	O(3)–Pb(3)–O(5)#6	70.7(4)
O(3)–Pb(2)–O(6)#5	157.4(4)	O(3)–Pb(3)–N(1)#4	144.4(5)
O(5)#3–Pb(2)–O(5)#6	136.2(4)	O(5)#6–Pb(3)–O(4)#4	79.4(4)
O(4)#4–Pb(3)–N(1)#4	81.3(6)	O(3)#4–Pb(3)–O(4)#4	47.8(4)

Symmetry codes: #1  $-x + 1, -y + 1, -z + 1$ ; #2  $x, -y + 1, z$ ; #3  $x + 1, y, z$ ; #4  $-x + 1, y, -z + 1$ ; #5  $-x + 1/2, -y + 3/2, -z + 1$ ; #6  $-x, y, -z + 1$ ; #7  $x + 1/2, -y + 3/2, z$ ; #8  $-x + 2, y, -z + 2$ .

**Table S2:**Selected bond lengths (Å) and angles (°) for  $\alpha$ -Pb(N<sub>3</sub>)<sub>2</sub>.

Pb(1)–N(4)	2.711(8)	Pb(1)–N(7)	2.632(7)
Pb(1)–N(6)#1	2.796(8)	Pb(1)–N(6)#2	2.695(8)
Pb(1)–N(10)	2.604(8)	Pb(1)–N(1)#1	2.896(4)
Pb(1)–N(7)#3	2.613(8)	Pb(1)–N(10)#3	2.753(8)
Pb(2)–N(3)	2.651(11)	Pb(2)–N(4)	2.578(8)
Pb(2)–N(9)#4	2.890(8)	Pb(2)–N(9)#2	2.890(8)
Pb(2)–N(1)#1	2.629(10)	Pb(2)–N(9)#5	2.833(8)
Pb(2)–N(9)#6	2.833(8)	Pb(2)–N(4)#7	2.578(8)
N(4)–Pb(1)–N(7)	78.3(2)	N(4)–Pb(1)–N(10)	78.5(2)
N(4)–Pb(1)–N(6)#1	120.2(2)	N(4)–Pb(1)–N(6)#2	84.3(2)
N(4)–Pb(1)–N(10)#3	134.5(2)	N(7)–Pb(1)–N(10)	68.7(3)
N(7)–Pb(1)–N(6)#1	135.1(2)	N(7)–Pb(1)–N(6)#2	74.7(2)
N(7)–Pb(1)–N(10)#3	126.9(2)	N(10)–Pb(1)–N(1)#1	79.5(3)
N(10)–Pb(1)–N(6)#2	141.9(2)	N(10)–Pb(1)–N(7)#3	99.3(2)
N(1)#1–Pb(1)–N(6)#1	85.7(2)	N(1)#1–Pb(1)–N(6)#2	124.4(3)
N(1)#1–Pb(1)–N(10)#3	69.8(3)	N(6)#1–Pb(1)–N(6)#2	67.9(2)
N(6)#1–Pb(1)–N(10)#3	71.5(2)	N(6)#2–Pb(1)–N(7)#3	83.2(2)
N(7)#3–Pb(1)–N(10)#3	66.7(2)	N(3)–Pb(2)–N(4)	73.6(2)
N(3)–Pb(2)–N(9)#5	136.65(18)	N(3)–Pb(2)–N(9)#4	68.8(2)
N(3)–Pb(2)–N(9)#6	136.65(18)	N(3)–Pb(2)–N(4)#7	73.6(2)
N(4)–Pb(2)–N(9)#5	78.9(2)	N(4)–Pb(2)–N(9)#4	141.5(2)
N(4)–Pb(2)–N(9)#6	144.6(2)	N(4)–Pb(2)–N(4)#7	99.1(3)
N(1)#1–Pb(2)–N(9)#4	138.44(17)	N(1)#1–Pb(2)–N(9)#2	138.44(17)
N(1)#1–Pb(2)–N(4)#7	73.9(2)	N(9)#5–Pb(2)–N(9)#4	124.8(2)
N(9)#5–Pb(2)–N(9)#6	82.9(2)	N(9)#5–Pb(2)–N(4)#7	144.6(2)
N(9)#4–Pb(2)–N(9)#6	73.2(2)	N(9)#4–Pb(2)–N(4)#7	78.2(2)
N(9)#2–Pb(2)–N(4)#7	141.5(2)	N(9)#6–Pb(2)–N(4)#7	78.9(2)
N(4)–Pb(1)–N(1)#1	67.7(3)	N(10)–Pb(1)–N(6)#1	149.4(2)
N(4)–Pb(1)–N(7)#3	156.1(2)	N(10)–Pb(1)–N(10)#3	78.3(3)
N(7)–Pb(1)–N(1)#1	137.3(2)	N(1)#1–Pb(1)–N(7)#3	135.8(2)
N(7)–Pb(1)–N(7)#3	78.7(2)	N(6)#1–Pb(1)–N(7)#3	73.2(2)

N(6)#2–Pb(1)–N(10)#3	134.8(2)	N(1)#1–Pb(2)– N(9)#5	71.7(2)
N(3)–Pb(2)–N(1)#1	128.9(3)	N(1)#1–Pb(2)–N(9)#6	71.7(2)
N(3)–Pb(2)–N(9)#2	68.8(2)	N(9)#5–Pb(2)–N(9)#2	73.2(2)
N(4)–Pb(2)–N(1)#1	73.9(2)	N(9)#4–Pb(2)–N(9)#2	80.9(2)
N(4)–Pb(2)–N(9)#2	78.2(2)	N(9)#2–Pb(2)–N(9)#6	124.8(2)

Symmetry codes: #1  $x - 1, y, z$ ; #2  $-x + 1, -y + 1, -z + 1$ ; #3  $x - 1/2, y, -z + 3/2$ ; #4  $-x + 1, -y + 1/2, -z + 1$ ; #5  $-x + 1/2, -y + 1, z - 1/2$ ; #6  $-x + 1/2, y + 1/2, z - 1/2$ ; #7  $x, -y + 3/2, z$ .



**Table S3:**Selected bond lengths (Å) and angles (°) for **Pb-FBA**.

Pb(1)–O(1)	2.293(3)	Pb(2)–O(3)#2	2.806(4)
Pb(1)–O(2)#1	2.554(5)	Pb(2)–O(1)	2.257(3)
Pb(1)–O(5)	2.435(5)	Pb(2)–O(1)#1	2.302(3)
Pb(1)–O(2)#3	2.800(4)	Pb(2)–O(3)	2.558(4)
Pb(1)–O(1)#1	2.307(3)	Pb(2)–O(4)	2.490(5)
O(1)–Pb(1)–O(5)	80.29(16)	O(1)–Pb(2)–O(3)#2	75.82(12)
O(1)–Pb(1)–O(2)#1	80.34(13)	O(3)–Pb(2)–O(3)#2	124.42(14)
O(5)–Pb(1)–O(2)#1	160.62(17)	O(4)–Pb(2)–O(1)#1	77.21(14)
O(1)#1–Pb(1)–O(2)#1	82.64(13)	O(1)–Pb(2)–O(3)	90.43(14)
O(1)–Pb(1)–O(2)#3	142.79(13)	O(1)–Pb(2)–O(1)#1	74.92(12)
O(5)–Pb(1)–O(2)#3	80.69(18)	O(3)–Pb(2)–O(1)#1	80.34(13)
O(2)#3–Pb(1)–O(1)#1	74.98(12)	O(3)#2–Pb(2)–O(1)#1	141.43(12)
O(1)–Pb(1)–O(1)#1	74.13(11)	O(1)–Pb(2)–O(4)	89.32(14)
O(5)–Pb(1)–O(1)#1	92.21(14)	O(3)–Pb(2)–O(4)	156.80(16)
O(2)#3–Pb(1)–O(2)#1	115.55(13)	O(4)–Pb(2)–O(3)#2	77.88(16)

Symmetry codes: #1  $-x + 5/4, y - 3/4, z + 1/4$ ; #2  $x + 3/4, -y + 5/4, z - 1/4$ ; #3  $-x + 1/2, -y + 2, z + 1/2$ .

**Table S4:**

The calculated interaction energies corrected with BSSE and ZPE,  $\Delta E_{\text{int}}$  for the associations **Pb**⋯**N<sub>3</sub>** and **Pb**⋯**4-FBN** (kcal·mol<sup>-1</sup>). Values listed in parentheses correspond to the values obtained based on the SMD solvation model.

Associations	$\Delta E_{\text{int}}$
<b>Pb</b> ⋯ <b>N<sub>3</sub></b>	-316.48 (-305.37)
<b>Pb</b> ⋯ <b>4-FBN</b>	-106.18 (-94.64)

**Table S5:**

Topological parameters at bond critical points of the Pb-N and N-N bonds in **MOF-N<sub>7</sub>'**

BCPs	$\rho(r)$	$\nabla^2\rho(r)$	$G(r)$	$V(r)$	$H(r)$	$ V(r) /G(r)$
Pb(1)⋯N(1)	0.028552	0.024241	0.012277	-0.018494	-0.006217	1.506394
Pb(3)⋯N(1)	0.018723	0.026135	0.008237	-0.009940	-0.001703	1.206750
N(1)⋯N(2)	0.434017	-0.829389	0.371937	-0.951221	-0.579284	2.557479
N(2)⋯N(3)	0.370128	-0.454354	0.266194	-0.645976	-0.379782	2.426711
N(3)⋯N(4)	0.556798	-1.459952	0.484983	-1.334954	-0.849971	2.752579

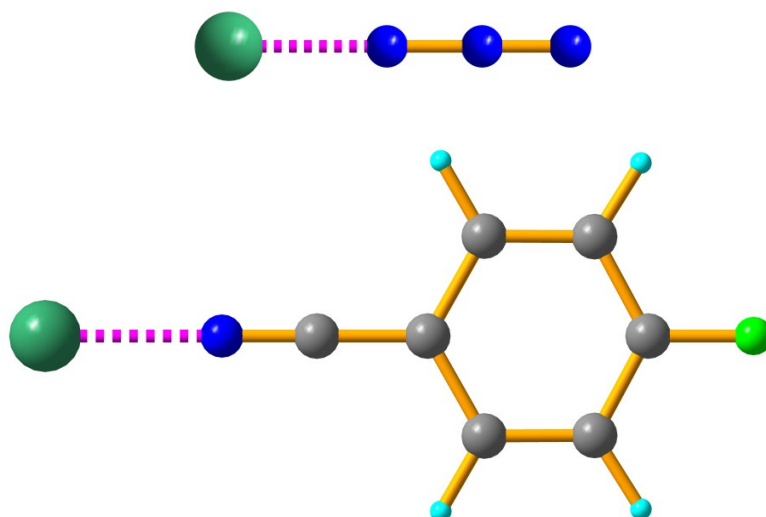


**Figure S1.** The calculated ground structures for the **Pb...N<sub>3</sub>** and **Pb...4-FBN** associations.

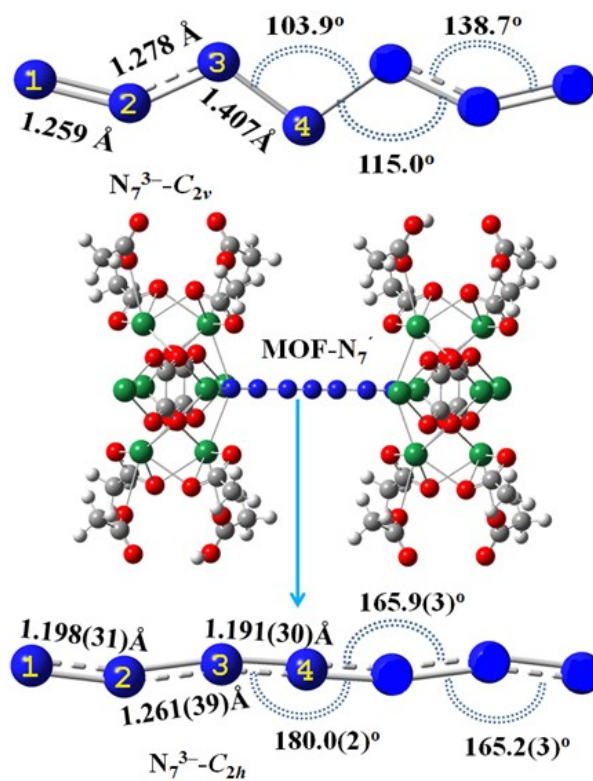


**Figure S2.** The structures of the representative fragments N<sub>7</sub><sup>3-</sup>-C<sub>2h</sub>, N<sub>7</sub><sup>3-</sup>-C<sub>2v</sub> and MOF-N<sub>7</sub>.

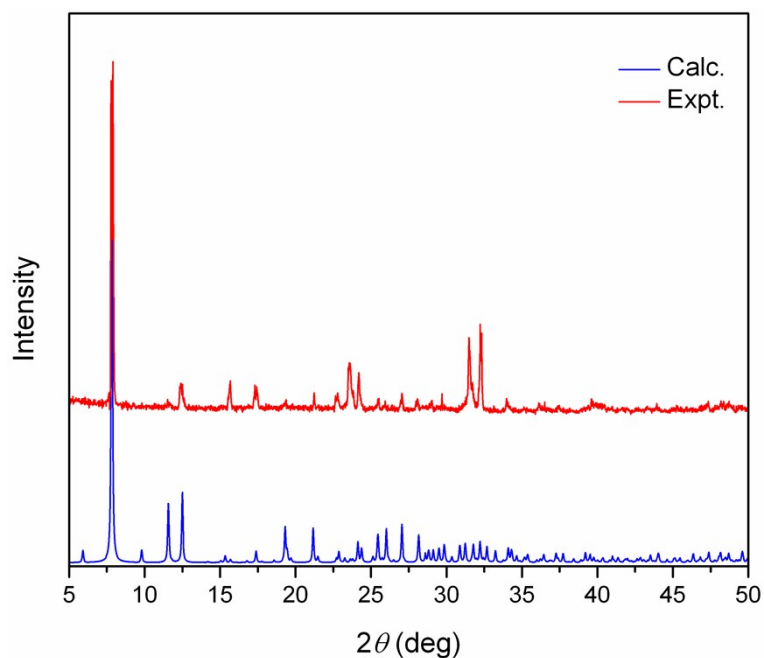


**Figure S3.** The XPRD patterns obtained for MOF-N<sub>7</sub>.

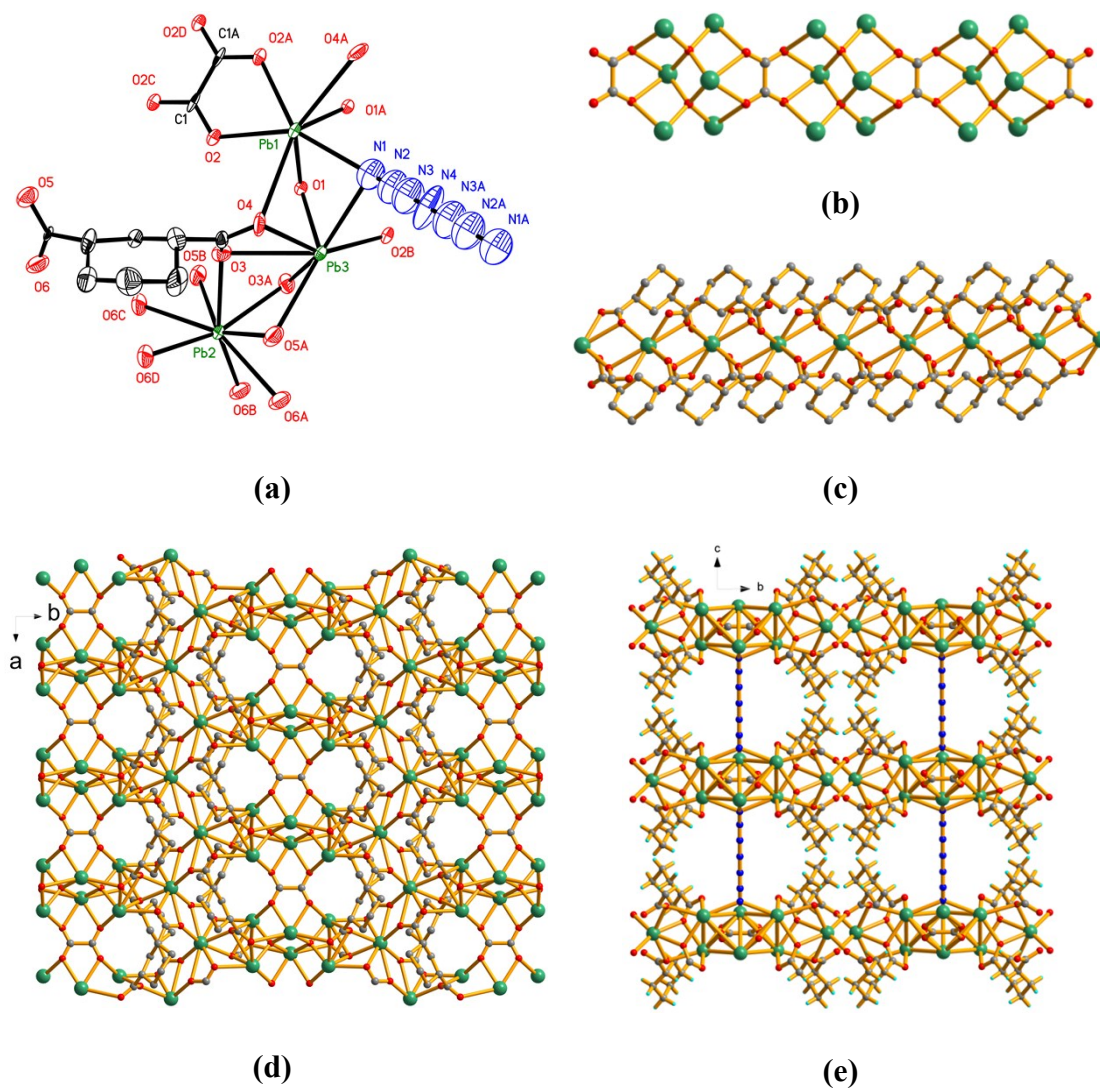


**Figure S4.** (a) The coordination environment of the Pb<sup>2+</sup> ions in **MOF-N<sub>7</sub>** with the ellipsoids drawn at the 30% probability level. Distorted water molecules and all hydrogen atoms were omitted for clarity. (b) The 1D chain constructed via the C<sub>2</sub>O<sub>4</sub><sup>2-</sup> anions and [Pb<sub>6</sub>O<sub>2</sub>]<sup>8+</sup> cationic clusters along the *a*-axis. (c) The 1D chain constructed via the CHDA<sup>2-</sup> anions and Pb<sup>2+</sup> ions along the *a*-axis. (d) The 2D metal-organic layer parallel to the *ab* plane in **MOF-N<sub>7</sub>**. (e) The 3D open framework constructed from the 2D layers and N<sub>7</sub> anionic pillars of **MOF-N<sub>7</sub>**.

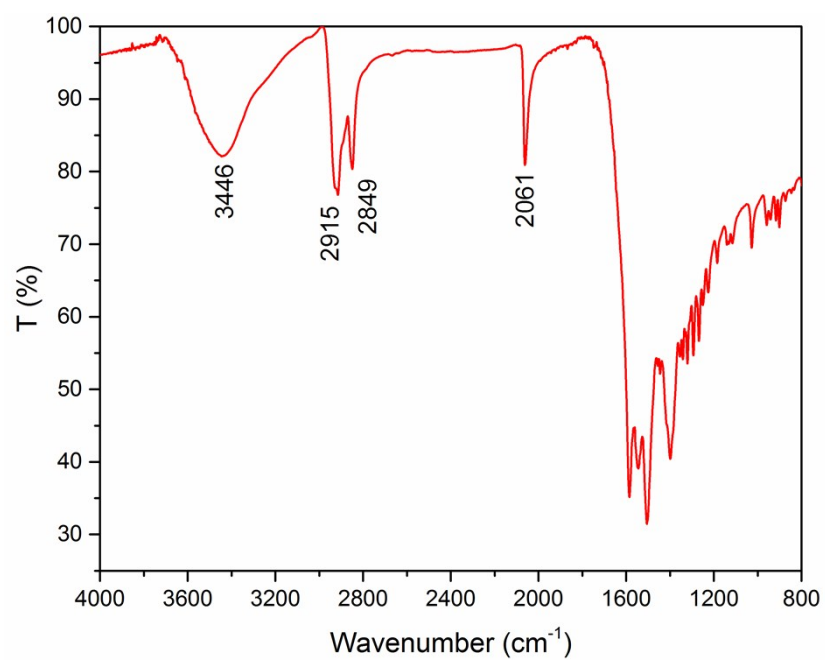


**Figure S5.** The FT-IR spectrum obtained of **MOF-N<sub>7</sub>**.

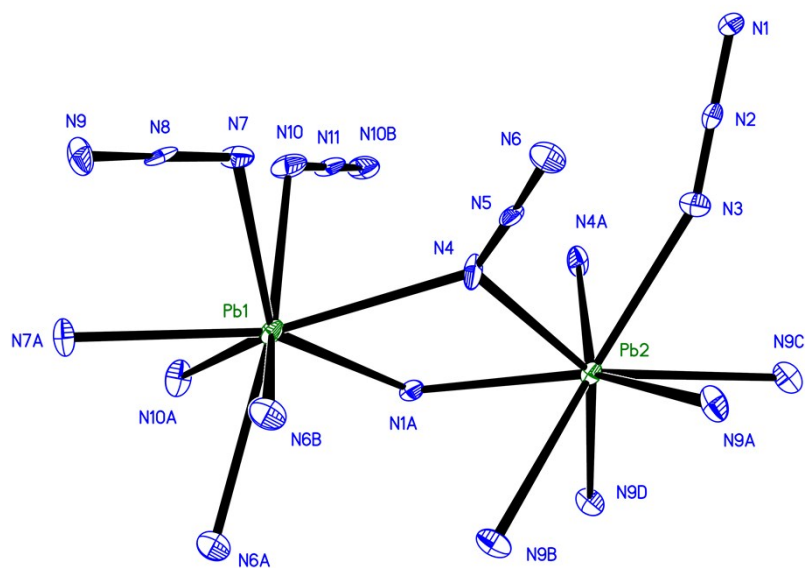


**Figure S6.** The coordination environment of the  $\text{Pb}^{2+}$  ions in  $\alpha\text{-Pb}(\text{N}_3)_2$  with the ellipsoids drawn at the 30% probability level.

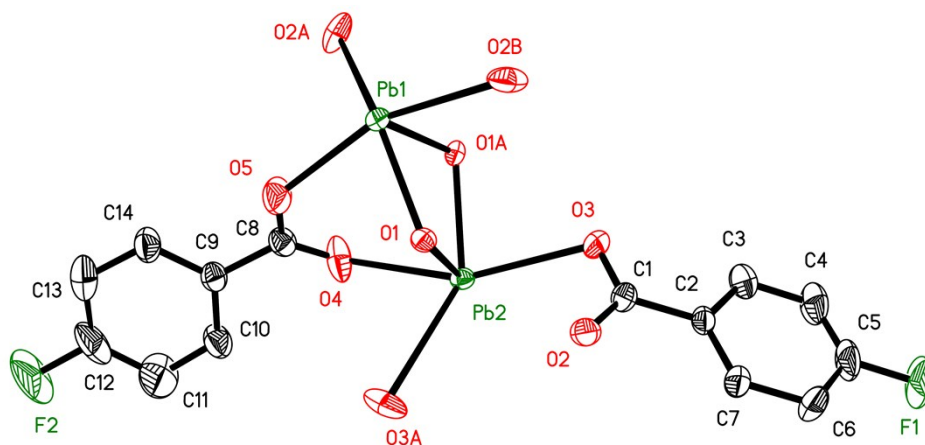


**Figure S7.** The coordination environment of the  $\text{Pb}^{2+}$  ion in **Pb-FBA** with the ellipsoids drawn at the 30% probability level. Distorted water molecules and all hydrogen atoms were omitted for clarity.



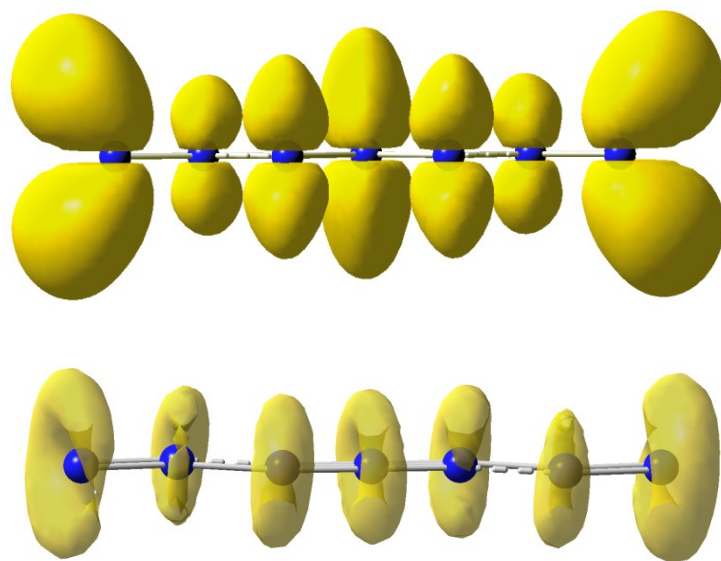


**Figure S8.** The ELF- $\pi$  isosurfaces (value = 0.70) of  $\text{N}_7^{3-}\text{-C}_{2v}$  (top) and the  $\text{N}_7^{3-}$  polynitrogen fragment in **MOF-N<sub>7</sub>'** (bottom).

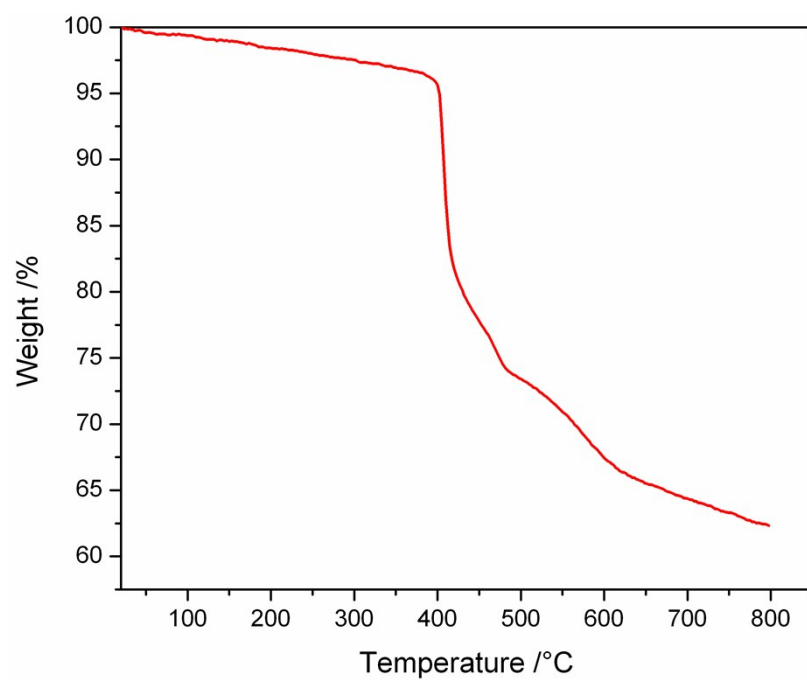


**Figure S9.** The TGA plot obtained for **Pb-FBA** at a heating rate of  $10^{\circ}\text{C}\cdot\text{min}^{-1}$  under a flow of  $\text{N}_2$ .